A Journal of the Gesellschaft Deutscher Chemiker

Angewandte Chemie

GDCh

International Edition

www.angewandte.org

Accepted Article

Title: A Photoswitchable Agonist for the Histamine H3 Receptor, a prototypic family A G protein-coupled receptor

Authors: Niels J. Hauwert, Tamara A.M. Mocking, Daniel Da Costa Pereira, Ken Lion, Yara Huppelschoten, Henry F. Vischer, Iwan J.P. De Esch, Maikel Wijtmans, and Rob Leurs

To be cited as: *Angew. Chem. Int. Ed.* 10.1002/anie.201813110
Angew. Chem. 10.1002/ange.201813110

Link to VoR: http://dx.doi.org/10.1002/anie.201813110
http://dx.doi.org/10.1002/ange.201813110

WILEY-VCH

10.1002/anie.201813110

COMMUNICATION

WILEY-VCH

A Photoswitchable Agonist for the Histamine H_3 Receptor, a prototypic family A G protein-coupled receptor

Niels J. Hauwert[+], Tamara A.M. Mocking[+], Daniel Da Costa Pereira, Ken Lion, Yara Huppelschoten, Henry F. Vischer, Iwan J.P. De Esch, Maikel Wijtmans*, Rob Leurs*

Abstract

Spatiotemporal control over biochemical signaling processes involving G protein-coupled receptors (GPCRs) is highly desired for dissecting their complex intracellular signaling. We developed a set of sixteen photoswitchable ligands for the human histamine H_3 receptor (hH_3R). Upon illumination key compound **65** decreases its affinity for the hH_3R 8.5-fold and its potency in hH_3R-mediated G_i protein activation over 20-fold, with the *trans* and *cis* isomer both acting as full agonist. Furthermore, in real-time two-electrode voltage clamp experiments in *Xenopus* oocytes, **65** shows rapid light-induced modulation of hH_3R activity. Ligand **65** shows good binding selectivity amongst the histamine receptor subfamily and has good photolytic stability. In all, **65** (VUF15000) is the first photoswitchable GPCR agonist confirmed to be modulated through its affinity and potency upon photoswitching while maintaining its intrinsic activity, rendering it a new chemical biology tool for spatiotemporal control of GPCR activation.

Introduction

In recent years, photopharmacology has been gaining momentum as a strategy to optically control biochemical processes.[1] The use of light as an external trigger to change ligand shape and consequently its pharmacological properties allows the probing of biological systems with great spatiotemporal resolution.[2] The azobenzene moiety is often used in photoswitchable ligands[1a] due to its limited size, high photostability and tunability of the peak absorption wavelength λ_{max}.[3] Its thermodynamically stable *trans* isomer typically involves a flat elongated structure, whereas its photoinduced *cis* configuration has a bent geometry with considerably shorter end-to-end distance.[4] Whereas photopharmacology is well established in the field of enzyme and ion channel modulation, it is an upcoming technology for G protein-coupled receptors (GPCRs).[1a] GPCRs constitute one of largest families of transmembrane proteins, their dysfunction is associated with a plethora of diseases and consequently GPCRs are one of the most successful classes of drug targets.[5] Recently, various GPCRs have been successfully targeted using photopharmacology approaches, including μ-opioid[6], CXCR3[7], CB1[8], H_3R[9], mGlu5[10] and GLP1[11]. Yet, almost all these examples include at least one but more frequently two antagonistic/partial agonist isomeric forms. In contrast, freely diffusible affinity and potency photoswitches in which both isomers act as full agonists are scarce[1a] even though such compounds would be very useful for photopharmacology approaches and complementary to agonist-to-antagonist switches.

The histamine H_3R receptor is an intensively studied GPCR that is known to play an important role in sleep disorders and cognition-related diseases such as Alzheimer's and Parkinson's disease. The first H_3R antagonist pitolisant (Wakix®) has been approved by the European Medicines Agency for the treatment of narcolepsy.[12] Recently, we published a toolbox of photoswitchable antagonists[9] that competitively inhibit histamine-induced H_3R activity. In the current work, we aimed to develop high-potency H_3R photoswitchable agonists that can simplify spatiotemporal studies of the signaling network of the H_3R. We disclose unique photoswitchable H_3R agonists that can be optically converted to isomers differing in their affinity and potency.

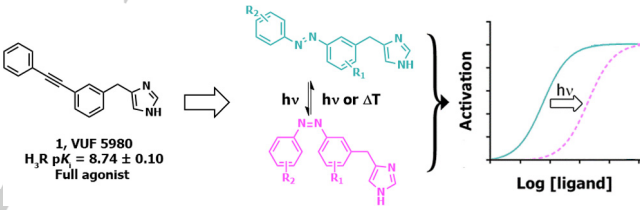

Figure 1. General design and concept of photoswitchable H_3R full agonists.

Main Text

The scaffold design was inspired by hH_3R full agonist VUF5980 previously published by our lab[13] (Figure 1). To date, virtually every published hH_3R full agonist contains a 4-substituted imidazole moiety combined with a basic or neutral side chain, as is the case for VUF5980. We left the imidazole portion of the molecule unchanged, and considered the diphenylacetylene moiety to be an attractive candidate for an "azologization" strategy.[3] Introducing the azobenzene at this position furthermore allows for great flexibility in the diversification of the scaffold. Based on the steep SAR observed with VUF5980[13] it was postulated that small changes would have significant impact on the affinity and potency for hH_3R. Therefore, primarily the azobenzene was decorated with small substituents (i.e. methyl and fluorine groups) on both phenyl rings.

[a] N.J. Hauwert MSc.*, T.A.M. Mocking MSc.*, D. Da Costa Pereira, Z. Lion MSc., Y. Huppelschoten MSc., Dr. H.F.Vischer, Prof. Dr. I.J.P.de Esch, Dr. M. Wijtmans, Prof. Dr. R. Leurs
* Authors contributed equally
Division of Medicinal Chemistry
Amsterdam Institute for Molecules Medicines and Systems (AIMMS)
Vrije Universiteit Amsterdam
De Boelelaan 1108, 1081 HZ, Amsterdam, The Netherlands
E-mail: M.Wijtmans@vu.nl, R.Leurs@vu.nl

Supporting information for this article is given via a link at the end of the document.

10.1002/anie.201813110

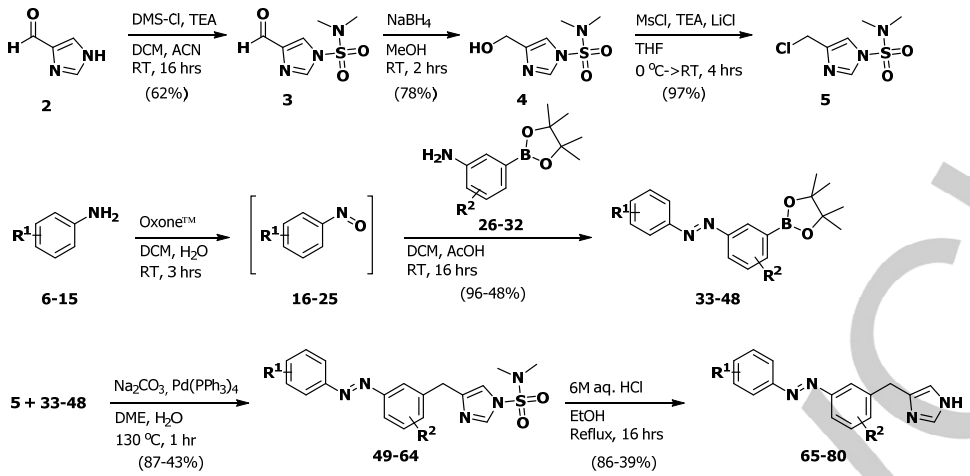

Scheme 1. General synthetic scheme for photoswitchable H_3R agonists. See supporting information for detailed experimental procedures

To synthesize the ligands, imidazole-4-carbaldehyde **2** was protected using *N,N*-dimethylsulfamoylchloride (DMS-Cl, Scheme 1) to afford **3**, which was reduced to **4**. Alcohol **4** was converted to chloride **5** using an *in situ* mesylation. A diverse set of anilines **6-15** was oxidized to the corresponding nitrosobenzenes **16-25** using Oxone™. After work-up, they were directly used in a Mills reaction with 3-amino-phenylboronic acid pinacol esters **26-32** to yield azobenzene-pinacol esters **33-48.** Cross coupling with chloride **5** yielded **49-64** in generally good yields. Acidic deprotection yielded final compounds **65-80** which were used for biological evaluation.

Compounds **65-80** all have λ_{max} values for the π-π^* transition of the *trans* isomer between 313 and 330 nm (Table 1). The observed limited variation is due to the absence of strong electron-donating or -withdrawing substituents. Similarly, λ_{max} values for the n-π^* transition of the *cis* isomer differed marginally, ranging between 417 and 430 nm. Upon continuous illumination with 360 ± 20 nm, the values for the photostationary states (PSS) of **65-80** ranged between 92.3 and 97.5% *cis*, except for **69** which has 82.6% *cis*. Compounds **65-80** all showed slow thermal relaxation at room temperature (20 °C, Table 1). The observed thermal relaxation half-lives were impractically long for direct quantification, therefore extrapolations of high temperature thermal relaxation were used to quantify half-lives at 20 °C (Table 1, Figure S1).[14] Compound **69** shows the fastest thermal relaxation in 50 mM Tris-HCl pH 7.4 buffer, having a half-life of 26.6 days, while **72** shows the slowest relaxation with a half-life of 147 days.

Based on its favorable pharmacological profile (vide infra) and synthetic tractability,

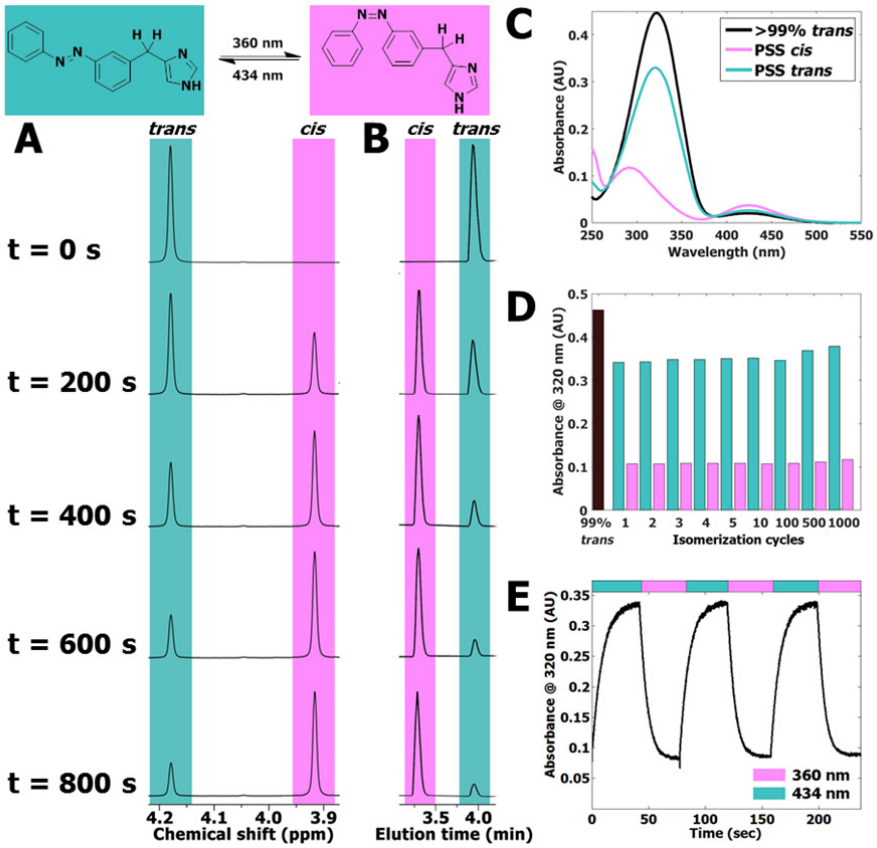

Figure 2: (A) Representative part of ^{1}H NMR spectra of 10 mM **65** in DMSO-d_6 illuminated at 360 ± 20 nm displayed at various time points (seconds). The presented peak belongs to the hydrogen atoms explicitly drawn in the structure shown above the spectrum. Full spectra are available in Figure S4. (B) Representative part of LC–MS chromatograms belonging to the illuminated NMR sample in Figure 2A. Full chromatograms are available in Figure S5. (C) UV–Vis spectra of 25 µM of **65** in 50 mM Tris–HCl pH 7.4 buffer + 1% DMSO-d_6. PSS *cis* represents a sample which has been illuminated for 300 s using 360 ± 20 nm light. PSS *trans* represents subsequent illumination for 300 s using 434 ± 9 nm. (D) Repeated isomerization of 25 µM of **65** in 50 mM Tris–HCl pH 7.4 buffer + 1% DMSO-d_6 analyzed at 320 nm. PSS *cis* was obtained by using illuminations for 40 s at 360 ± 20 nm. PSS *trans* was obtained by using illuminations for 40 s at 434 ± 9 nm. (E) Absorbance at 320 nm of 25 µM of **65** in 50 mM Tris–HCl pH 7.4 buffer + 1% DMSO-d_6. UV–Vis spectra were obtained with 1 s intervals under alternating illumination with 360 ± 20 nm and 434 ± 9 nm perpendicular to the light source of the UV–Vis spectrometer.

compound **65** was subjected to in-depth photochemical characterization using ^{1}H-NMR and LC-MS analysis during illumination with 360 ± 20 nm. The well-resolved signal of the benzylic CH_2 group provided a clear handle for quantification in ^{1}H-NMR analysis (Figure 2A). An overestimation of isomerization percentage is observed in LCMS analysis at 254 nm compared to ^{1}H-NMR analysis (Figure 2B, Table S1), which can be explained by the differences in extinction coefficients for the *trans* and *cis* isomer at 254 nm (Figure 2C, S2, S3). Compound **65** shows excellent resistance to photobleaching upon >1000 times isomerization (Figure 2D). The dynamic isomerization was studied using UV-Vis spectroscopy under alternating illumination (Figure 2E). At 25 µM of **65** in 50 mM Tris-HCl pH 7.4 buffer + 1% DMSO-d_6, a half-life of 4.2 ± 0.16 s for 360 ± 20 nm and 5.7 ± 0.19 s for 434 ± 9 nm was observed.

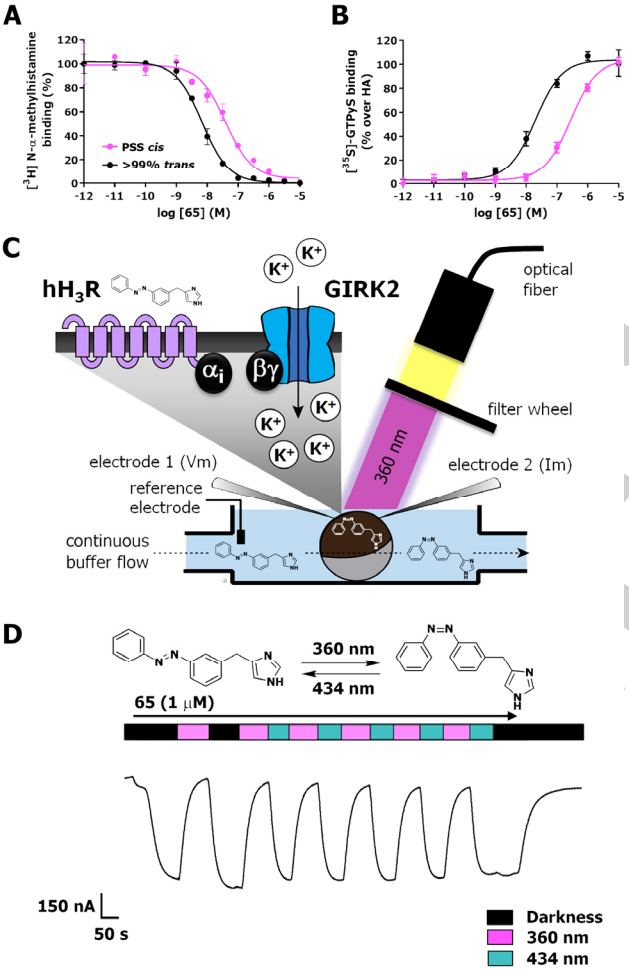

Figure 3. Representative curves of **65** (A) in competition binding with [^{3}H]-NAMH or (B) in G_i protein activation as measured by [^{35}S]-GTPγS accumulation on HEK293T cell homogenates transiently expressing hH_3R. Black lines refer to a sample containing >99% *trans*, while magenta lines refer to a sample illuminated to PSS with 360 ± 20 nm prior to the assay. (C) Schematic drawing of the TEVC setup used for dynamic hH_3R and GIRK current activation in *Xenopus laevis* oocytes expressing hH_3R and GIRK. (D) Representative part of a GIRK-mediated current trace during continuous perfusion with 1 µM **65** under illumination of the oocyte with alternating 360 ± 20 and 434 ± 9 nm wavelength as measured by TEVC. Error bars shown are mean ± SD.

The long thermal relaxation half-lives allowed for detailed pharmacological evaluation using hH_3R competition binding as well as functional experiments. For this, the compound solutions were either illuminated using 360 ± 20 nm to reach a PSS *cis* or kept in the dark to ensure >99% *trans* isomer. Then, the affinity of both isomers for the hH_3R was assessed in competition binding with [^{3}H]-N$^\alpha$-methylhistamine (NAMH). All compounds display hH_3R binding affinity, which decreases upon illumination reaching up to a 21-fold affinity difference in the case of **76**. In terms of absolute affinity, **65** displays the highest affinities for the hH_3R with a pK_i value of 8.42 ± 0.04 for its *trans* isomer and a pK_i of 7.49 ± 0.05 for its *cis* isomer, resulting in an 8.5-fold shift upon illumination (Figure 3A, Table 1). Fluorine-substituted analogues **67** and **80** perform similarly to **65** in competition binding displaying only a marginally lower affinity (Table 1). Notably, *para*-methyl substitution on the R^1 position (**78**) decreases the binding affinity and abrogates the photoisomerization induced affinity shift compared to **65** (Table 1). Reduction of the size of the *para*-substituents to either chlorine (**71**) or fluorine (**68**) gradually rescues hH_3R affinity and reestablishes the shift in affinity to 6- and 15-fold, respectively. Methyl addition to either the *ortho* (**76**) or *meta* (**77**) position of R^1 still results in decent binding affinities and high (21-fold) to good (8.5-fold) affinity shifts upon illumination. Addition of substituents at the R^2 position results in a clear affinity cliff, with fluorine substitutions (**79** and **80**) still being allowed, but addition of a methyl substituent (**72**-**75**) highly decreased the binding affinity of the *cis* isomer. Moreover, for the *trans* isomers, 4-Me (**73**) and 6-Me (**75**) substitution is still tolerated yet showing a log-unit decrease in hH_3R affinity compared to **65**, while 2-Me (**72**) and 5-Me (**74**) groups highly reduce hH_3R affinity and consequently reduce or even abolish (**72**) the affinity shift (Table 1).

Based on the observed affinities and photo-induced affinity shifts, the efficacy to stimulate hH_3R-mediated G_i protein activation was evaluated for ligands **65** and **76** in a [^{35}S]-GTPγS binding assay. Highest affinity ligand **65** (pK_i *trans* = 8.42 ± 0.04) also displays the highest potency (pEC_{50} *trans* = 7.60 ± 0.13) to induce G_i activation, which upon photoisomerization decreases 20-fold (pEC_{50} at PSS *cis*: 6.30 ± 0.13) with both isomers being full agonists with both having intrinsic activities of α = 1.0 ± 0.03, as compared to histamine (Figure 3B). Since the observed shift in hH_3R affinity was 8.5-fold, the larger (20-fold) shift in functional potency indicates that for **65** the efficacy (propensity to activate a GPCR[15]) is also affected upon *trans-cis* isomerization. Interestingly, a large photo-induced decrease in potency of 23-fold was also obtained for **76** (pEC_{50} *trans*: 6.78 ± 0.11, PSS *cis*: 5.41 ± 0.11, α = 1.00 ± 0.0). This shift in potency of **76** is completely explained by the observed change of its affinity (vide supra).

Compound **65** (VUF15000) was selected as tool compound for further analysis as it has good synthetic tractability and because its superior potency is a clear advantage for pharmacological studies. As the imidazole-based pharmacophore/scaffold used in the design of these photoswitchable ligands is prone to interact with other histamine receptor subtypes[13], **65** was tested for its subtype selectivity. Binding of **65** is >300-fold selective for hH_3R over hH_1R and hH_2R (Table S2), while a 31-fold selectivity is observed over its

closest homologue hH_4R (Table S2). Interestingly, **65** displays high nM (*trans*) to low µM (PSS *cis*) binding affinities for both mouse and rat H_3R with a 4-fold and 8-fold shift in binding affinity upon photoisomerization, respectively (Table S2).

Real-time photomodulation of hH_3R activity by **65** was measured using two-electrode voltage clamp (TEVC) on *Xenopus laevis* oocytes expressing both hH_3R and G protein-coupled inwardly-rectifying potassium (GIRK)-channels (Figure 3C). In this expression system, histamine application results in hH_3R-mediated GIRK activation, which is insensitive to optical modulation.[9] As expected based on our data with the [^{35}S]-GTPγS binding assay, *trans*-**65** elicits an agonistic response in this system, which could be reduced by switching to the less active *cis* isomer upon illumination with 360 ± 20 nm. Retrieval of the agonistic response could be provoked by either actively switching the *cis* isomer back into its *trans* isomer by illuminating with 434 ± 9 nm or by stopping illumination, due to continuous perfusion of the *trans* isomer (Figure 3D). Dynamic photoswitching of **65** could be performed repeatedly, illustrating that the use of two specific wavelengths allows optical control of the hH_3R activation mediated by **65**. Furthermore, photoswitchable agonist **65** shows rapid hH_3R activation and deactivation kinetics, aiding in its use in in vivo experimentation.

Conclusion

We have synthesized and characterized 16 photoswitchable hH_3R agonists that change their affinity and potency upon illumination, indicating a successful azologization strategy. All possess long thermal relaxation half-lives at room temperature making them useful for a variety of pharmacological studies. Compound **65** (VUF15000) was selected as key compound on the basis of synthetic tractability and highest absolute hH_3R affinity. Moreover, upon illumination **65** displays a high potency and 20-fold potency shift while maintaining full intrinsic activity in G_i protein activation making it especially attractive as a tool compound. With a 20-fold shift in potency, **65** is one of the best photoswitchable GPCR agonists reported so far. Electrophysiology experiments showed the dynamic optical modulation of hH_3R activation induced by **65** in real time, setting the stage for further unraveling of the downstream signaling of hH_3R with great spatiotemporal precision. Recently, photopharmacology approaches with freely diffusible GPCR ligands have for the first time been used successfully in vivo to modulate tadpole and zebrafish behavior[10, 16] and to elucidate the role of the metabotropic glutamate receptor 4 in the nervous system using a mouse model of chronic pain.[17] In view of the widespread distribution of the H_3R in the central and peripheral nervous system, photopharmacology approaches with tools such as **65** offer new means (complimentary to optogenetic approaches[18]) to investigate the spatial and temporal details of H_3R modulation of important processes like arousal, cognition and neuropathic pain.[12a-e]

10.1002/anie.201813110

Table 1. Structure-affinity relationship of photoswitchable azobenzene-derived H_3R agonists.

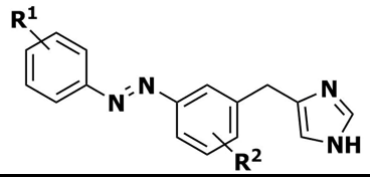

Compound number	R^1	R^2	pK_i *trans* ± SEM	pK_i at PSS *cis*[a] ± SEM	pK_i shift ± SEM	λ_{max} *trans*[b] (nm)	λ_{max} *cis*[b] (nm)	$t_{1/2}$[c] (days)	PSS[d] ± SEM
1	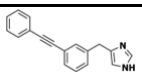		8.74 ± 0.10[a]		-	-	-	-	-
65	H	H	8.42 ± 0.04	7.49 ± 0.05	-0.93 ± 0.06	320	427	106	96.1 ± 1.9
66	2-F	H	8.28 ± 0.08	7.09 ± 0.03	-1.19 ± 0.04	323	425	128	95.7 ± 0.27
67	3-F	H	8.35 ± 0.09	7.42 ± 0.05	-0.93 ± 0.04	320	425	101	94.1 ± 1.3
68	4-F	H	7.69 ± 0.08	6.51 ± 0.08	-1.18 ± 0.09	322	426	95.9	95.9 ± 1.6
69	2,6-F	H	8.00 ± 0.02	7.26 ± 0.09	-0.74 ± 0.10	313	417	26.6	82.6 ± 1.9
70	2-Cl	H	7.86 ± 0.03	6.85 ± 0.04	-1.02 ± 0.03	324	420	96.1	95.3 ± 0.22
71	4-Cl	H	6.76 ± 0.07	5.98 ± 0.07	-0.78 ± 0.10	326	428	29.7	97.5 ± 0.48
72	H	2-Me	5.57 ± 0.09	5.45 ± 0.03	-0.12 ± 0.10	323	428	147	92.3 ± 4.9
73	H	4-Me	6.90 ± 0.06	5.77 ± 0.13	-1.13 ± 0.08	327	430	42.9	96.3 ± 1.1
74	H	5-Me	5.75 ± 0.03	5.13 ± 0.17	-0.62 ± 0.19	322	427	122	94.5 ± 1.4
75	H	6-Me	7.15 ± 0.03	5.94 ± 0.06	-1.21 ± 0.04	324	426	125	95.8 ± 0.92
76	2-Me	H	7.72 ± 0.03	6.40 ± 0.04	-1.32 ± 0.05	326	426	35.6	96.5 ± 1.6
77	3-Me	H	7.39 ± 0.08	6.46 ± 0.06	-0.94 ± 0.09	323	428	77.0	95.4 ± 0.39
78	4-Me	H	5.72 ± 0.14	5.71 ± 0.06	-0.01 ± 0.16	330	429	34.1	94.0 ± 4.4
79	H	4-F	7.81 ± 0.07	6.54 ± 0.06	-1.27 ± 0.02	324	425	91.7	96.6 ± 0.51
80	H	6-F	8.39 ± 0.06	7.36 ± 0.03	-1.03 ± 0.03	322	427	84.6	94.6 ± 1.3

[a] Adapted from Wijtmans *et al.*[13] [b] Determined at 25 μM in 50 mM Tris-HCl pH 7.4 buffer + 1% DMSO-d_6. [c] Thermal relaxation half-life times as determined according to the method of Priimagi et al.[14] in 50 mM Tris-HCl pH 7.4 buffer + 1% DMSO-d_6 extrapolating to 20 °C. Arrhenius plots are available in Figure S1. [d] Photostationary state area percentages after illumination with 360 ± 20 nm at 1 mM in DMSO-d_6 and as determined by LC−MS analysis at 254 nm. All pharmacology experiments were at least performed as triplicate.

Acknowledgements

We acknowledge The Netherlands Organisation for Scientific Research (NWO) for financial support (TOPPUNT, "7 ways to 7TMR modulation (7-to-7)", 718.014.002). All authors participate in the European Cooperation in Science and Technology Action CM1207 [GPCR-Ligand Interactions, Structures, and Transmembrane Signaling: A European Research Network (GLISTEN)]. We thank Hans Custers for HRMS analyses, Andrea van de Stolpe for setting up the photochemistry equipment and Fons Lefeber (Leiden University) for NMR assistance. Kristoffer Sahlholm (Karolinska institute) is kindly acknowledged for providing the pcDNA3.1-Kir3.1 and -Kir3.4 plasmids.

Keywords: Photopharmacology • VUF15000 • H_3R • Agonism • Dynamic modulation

[1] a) K. Hull, J. Morstein, D. Trauner, *Chem. Rev.* **2018**, *118*, 10710-10747; b) M. W. H. Hoorens, W. Szymanski, *Trends Biochem. Sci.* **2018**, *43*, 567-575.

[2] W. Szymanski, J. M. Beierle, H. A. Kistemaker, W. A. Velema, B. L. Feringa, *Chem. Rev.* **2013**, *113*, 6114-6178.

[3] J. Broichhagen, J. A. Frank, D. Trauner, *Acc. Chem. Res.* **2015**, *48*, 1947-1960.

[4] A. A. Beharry, G. A. Woolley, *Chem. Soc. Rev.* **2011**, *40*, 4422-4437.

[5] a) A. S. Hauser, S. Chavali, I. Masuho, L. J. Jahn, K. A. Martemyanov, D. E. Gloriam, M. M. Babu, *Cell* **2018**, *172*, 41-54 e19; b) K. Sriram, P. A. Insel, *Mol. Pharmacol.* **2018**, *93*, 251-258.

[6] M. Schönberger, D. Trauner, *Angew. Chem. Int. Ed. Engl.* **2014**, *53*, 3264-3267.

[7] X. Gomez-Santacana, S. M. de Munnik, P. Vijayachandran, D. Da Costa Pereira, J. P. M. Bebelman, I. J. P. de Esch, H. F. Vischer, M. Wijtmans, R. Leurs, *Angew. Chem. Int. Ed. Engl.* **2018**, *57*, 11608-11612.

[8] M. Westphal, M. A. Schafroth, R. Sarott, M. Imhof, C. Bold, P. Leippe, A. Dhopeshwarkar, J. Grandner, V. Katritch, K. Mackie, D. Trauner, E. M. Carreira, J. A. Frank, *J. Am. Chem. Soc.* **2017**, *139*, 18206-18212.

[9] N. J. Hauwert, T. A. M. Mocking, D. Da Costa Pereira, A. J. Kooistra, L. M. Wijnen, G. C. M. Vreeker, E. W. E. Verweij, A. H. De Boer, M. J. Smit, C. De Graaf, H. F. Vischer, I. J. P. de Esch, M. Wijtmans, R. Leurs, *J. Am. Chem. Soc.* **2018**, *140*, 4232-4243.

[10] S. Pittolo, X. Gomez-Santacana, K. Eckelt, X. Rovira, J. Dalton, C. Goudet, J. P. Pin, A. Llobet, J. Giraldo, A. Llebaria, P. Gorostiza, *Nat. Chem. Biol.* **2014**, *10*, 813-815.

[11] J. Broichhagen, T. Podewin, H. Meyer-Berg, Y. von Ohlen, N. R. Johnston, B. J. Jones, S. R. Bloom, G. A. Rutter, A. Hoffmann-Roder, D. J. Hodson, D. Trauner, *Angew. Chem. Int. Ed. Engl.* **2015**, *54*, 15565-15569.

[12] a) R. Leurs, R. A. Bakker, H. Timmerman, I. J. P. de Esch, *Nat. Rev. Drug Discov.* **2005**, *4*, 107-120; b) P. Panula, P. L. Chazot, M. Cowart, R. Gutzmer, R. Leurs, W. L. Liu, H. Stark, R. L. Thurmond, H. L. Haas, *Pharmacol. Rev.* **2015**, *67*, 601-655; c) M. A. Khanfar, A. Affini, K. Lutsenko, K. Nikolic, S. Butini, H. Stark, *Front. Neurosci.* **2016**, *10*, 201; d) P. Panula, S. Nuutinen, *Nat. Rev. Neurosci.* **2013**, *14*, 472-487; e) E. Tiligada, K. Kyriakidis, P. L. Chazot, M. B. Passani, *CNS Neurosci. Ther.* **2011**, *17*, 620-628; f) M. Kollb-Sielecka, P. Demolis, J. Emmerich, G. Markey, T. Salmonson, M. Haas, *Sleep Med.* **2017**, *33*, 125-129.

[13] M. Wijtmans, S. Celanire, E. Snip, M. R. Gillard, E. Gelens, P. P. Collart, B. J. Venhuis, B. Christophe, S. Hulscher, H. van der Goot, F. Lebon, H. Timmerman, R. A. Bakker, B. I. Lallemand, R. Leurs, P. E. Talaga, I. J. P. de Esch, *J. Med. Chem.* **2008**, *51*, 2944-2953.

[14] Z. Ahmed, A. Siiskonen, M. Virkki, A. Priimagi, *Chem. Commun.* **2017**, *53*, 12520-12523.

[15] T. P. Kenakin, *Pharmacologic analysis of drug-receptor interaction*, 2nd ed., Raven

Press, New York, United States of America, **1993**.

[16] X. Gomez-Santacana, S. Pittolo, X. Rovira, M. Lopez, C. Zussy, J. A. Dalton, A. Faucherre, C. Jopling, J. P. Pin, F. Ciruela, C. Goudet, J. Giraldo, P. Gorostiza, A. Llebaria, *ACS Cent. Sci.* **2017**, *3*, 81-91.

[17] C. Zussy, X. Gomez-Santacana, X. Rovira, D. De Bundel, S. Ferrazzo, D. Bosch, D. Asede, F. Malhaire, F. Acher, J. Giraldo, E. Valjent, I. Ehrlich, F. Ferraguti, J. P. Pin, A. Llebaria, C. Goudet, *Mol. Psychiatry* **2018**, *23*, 509-520.

[18] R. H. Williams, M. J. Chee, D. Kroeger, L. L. Ferrari, E. Maratos-Flier, T. E. Scammell, E. Arrigoni, *J. Neurosci.* **2014**, *34*, 6023-6029.

10.1002/anie.201813110

WILEY-VCH

Entry for the Table of Contents

COMMUNICATION

Shedding light on G protein-coupled receptor activation: VUF15000 is a photoswitchable histamine H_3 receptor agonist showing full G_i protein activation in both its *trans* and *cis* isomer. Moreover, it shows dynamic optical H_3 receptor modulation in electrophysiology experiments. VUF15000 can serve as a valuable photochromic tool compound for unraveling the H_3 receptor signaling cascade with spatiotemporal precision.

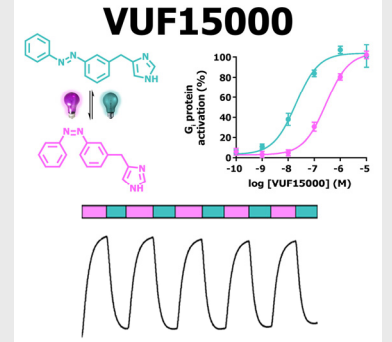

Photochromic agonist for H_3 receptor signaling

Niels J. Hauwert[+], Tamara A.M. Mocking[+], Daniel Da Costa Pereira, Ken Lion, Yara Huppelschoten, Henry F. Vischer, Iwan J.P. De Esch, Maikel Wijtmans, Rob Leurs**

Page No. – Page No.

A Photoswitchable Agonist for the Histamine H_3 Receptor, a prototypic family A G protein-coupled receptor